Analytica Chimica Acta 888 (2015) 44–51

Contents lists available at ScienceDirect

Analytica Chimica Acta

journal homepage: www.elsevier.com/locate/aca

Sensor–actuator system for dynamic chloride ion determination

Derk Balthazar de Graaf, Yawar Abbas*, Johan Gerrit Bomer, Wouter Olthuis, Albert van den Berg

BIOS-Lab on a Chip Group, MESA+ Institute for Nanotechnology, MIRA Institute for Biomedical Technology and Technical Medicine, University of Twente, 7500AE Enschede, The Netherlands

HIGHLIGHTS

- Concentration of Cl^- is measured using the transition time of a Ag/AgCl electrode.
- Sensor electrode detects the Cl^- resulting from the current applied to the actuator.
- The square root of the transition time is proportional to the [Cl^-] at the sensor.
- Any metal wire can be used as a pseudo-reference electrode.
- Long-term stable measurements as compare to combined sensor–actuator.

GRAPHICAL ABSTRACT

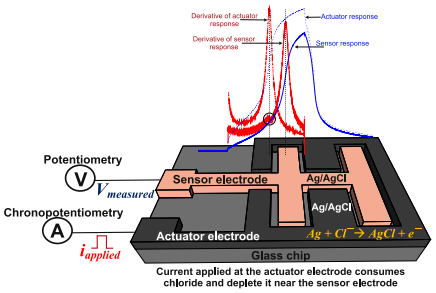

ARTICLE INFO

Article history:
Received 7 April 2015
Received in revised form
10 June 2015
Accepted 12 June 2015
Available online 7 August 2015

Keywords:
Chronopotentiometry
Chloride ion measurement
Silver/silver chloride electrode
Transition time
Separated sensor–actuator
Pseudo-reference electrode

ABSTRACT

Chloride is a crucial anion for various analytical applications from biological to environmental applications. In order to measure the chloride ion concentration, a measurement system is needed which can detect this concentration for prolonged times reliably. Chronopotentiometry is a technique which does not need a long term stable reference electrode and is therefore very suitable for prolonged ion concentration measurements. As the used electrode might be fouled by reaction products, this work focuses on a chronopotentiometric approach with a separated sensing electrode (sensor) and actuating electrode (actuator). Both actuation and sensor electrode are made of Ag/AgCl. A constant current is applied to the actuator and will start the reaction between Ag and Cl^-, while the resulting Cl^- ion concentration change is observed through the sensor, which is placed close to the actuator. The time it takes to locally deplete the Cl^- ions is called transition time. Experiments were performed to verify the feasibility of this approach. The performed experiments show that the sensor detects the local concentration changes resulting from the current applied to the actuator. A linear relation between the Cl^- ion concentration and the square root of the transition time was observed, just as was predicted by theory. The calibration curves for different chips showed that both a larger sensor and a larger distance between sensor and actuator resulted in a larger time delay between the transition time detected at the actuator and the sensor.

1. Introduction

Chloride ion concentration is an important parameter for various biological and environmental applications [1,2]. Chloride is a key parameter of water quality and salinity [3]. In mechanical

Abbreviations: RE, reference electrode; WE, working electrode; CE, counter electrode; AE, actuator electrode; SE, sensor electrode; ISFET, ion-selective field-effect transistor; BHF, buffered hydrogen fluoride.

* Corresponding author. University of Twente, BIOS Chair, Carre 2247, P.O. Box 217, 7500 AE Enschede, The Netherlands.
E-mail address: y.abbas@utwente.nl (Y. Abbas).

http://dx.doi.org/10.1016/j.aca.2015.06.047
0003-2670/

industries chloride is a major contributor to corrosion of metal components in steam-generating systems [1]. Chloride is also one of the major contributors to reinforcement corrosion in concrete, especially for structures near sea water or which are exposed to deicing salt [4,5]. The chloride ion concentration inside the reinforced concrete has been linked to the corrosion process and it is therefore highly desirable to be able to detect the chloride ion concentration level [6–8]. Thus, keeping in view these applications, the development of a long-term and reliable chloride ion sensor is of great importance.

In recent years many groups have investigated the in situ measurement of chloride in concrete using mainly chemical [9,10], electrochemical [11–13] and optical methods [1]. Optical techniques lacks the selectivity, compactness and convenience, whereas chemical techniques are tiresome and labor intensive. On the other hand electrochemical techniques are selective, fast and reliable [11]. In electrochemical techniques, potentiometry is commonly used to determine chloride concentrations, but this technique needs a stable (liquid junction) reference electrode [6,12]. Such electrodes are relatively fragile and often need regular recalibration, making long-term reliable measurements impossible [11,13].

A dynamic electrochemical measurement technique, such as chronopotentiometry, can overcome these drawbacks [14–17]. In chronopotentiometry, the potential of an electrode is measured while a current pulse is applied. Due to the depletion of ions present in the solution, the resulting chronopotentiogram will show an inflection point [18,19] when the concentration of a specific ion reaches zero at the surface of the electrode and secondary ions will start carrying the current [20–22]. The point in time at which this inflection occurs is a measure for the ion concentration [21]. Since the point in time of the inflection point in the chronopotentiogram is used and not the measured (absolute) potential itself, the reference electrode has less strict requirements and any metal wire can be used as a pseudo-reference electrode [21,23]. Abbas et al. previously showed that chronopotentiometry can successfully be applied as a means to determine chloride ion concentration levels by the use of a Ag/AgCl working electrode [21].

However, during the measurement cycle, the surface of Ag/AgCl is degraded due to the applied current pulse. After the Cl^- concentration is depleted at the electrode, other ions present in the solution will interact with the electrode, especially oxygen, forming Ag_2O [21,24]. These unwanted reactions, change the surface of the electrode, which influence the measurement results. To overcome this problem, the functions performed during chronopotentiometry can be divided over two electrodes, i.e. one electrode (called 'actuating electrode' or 'actuator') will carry the (constant) current and make sure that a constant amount of ion conversions is done while the potential is measured at a second (non-current carrying) electrode (called 'sensing electrode' or 'sensor'). The separated sensor and actuator approach has been previously used by Olthuis et al. in ISFET for measuring the pH [25,26]. This work investigates the feasibility of such a separated sensor–actuator system for the detection of chloride ions with the use of Ag/AgCl electrodes.

2. Theory

The observed electrode potential of a Ag/AgCl working electrode is a function of the chloride ion concentration as described by the Nernst equation [23,27]. By applying an anodic current pulse to the Ag/AgCl electrode, a faradaic reaction takes place at the electrode surface:

$$Ag + Cl^- \rightarrow AgCl + e^- \quad (1)$$

Due to the consumption of Cl^- ion its concentration changes consequently changing the half-cell potential (or potential response) of the Ag/AgCl electrode, see Fig. 1. After some time, the Cl^- ion concentration at the electrode surface will deplete and ultimately drop to zero. At this point, the flux of Cl^- ions toward the electrode is no longer sufficient to supply all electrons needed to sustain the applied current. This results in a potential shift to a higher value (visible in Fig. 1b) where another faradaic reaction occurs, e.g. the reaction with oxygen present in the solution to form silver oxide [21].

The time at which the ions deplete completely near the electrode surface is called transition time (τ) [21,23]. For a constant current pulse, this τ can be calculated using the Sand equation:

$$\tau = \frac{D_{Cl^-}\pi}{4}\left(\frac{FAC^*_{Cl^-}}{I}\right)^2 \quad (2)$$

where D_{Cl^-} is the diffusion coefficient, F is Faraday's constant, A is the electrode area, $C^*_{Cl^-}$ is the initial ion concentration and I the applied current. By deriving the transition time from a chronopotentiogram, the initial Cl^- ion concentration can be calculated [11].

As the faradaic reaction eq. (1) consumes silver from the electrode, the working electrode is prone to fouling over time. Furthermore, the potential shift can only be observed after the second faradaic reaction has started, changing the electrode surface even further. By separating the actuation and sensing function of the electrode into two separate electrodes, precipitation on the current carrying electrode does no longer influence the (chrono) potentiometric measurements. The sensing electrode (SE) can be a purely, almost zero-current potentiometric device, preventing fouling of the SE and reducing the potential drop between the SE and reference electrode often visible at current carrying electrodes. Another electrode, called actuating electrode (AE) is used to carry the current and deplete the Cl^- ion concentration at its surface.

Fig. 2 shows a schematic representation of the sensing system. As can be seen, a current is applied through the AE with respect to a counter electrode (CE). The potential is measured at the SE versus a reference electrode (RE). As the transition time is derived from a potential shift and not determined by an absolute potential value, the demands for the stable RE are lower than would be necessary in normal potentiometry: the reference potential should only be stable during the measurement, i.e. changes in reference potential are no problem as long as they do not occur within the measurement time frame (typically seconds).

3. Experimental

3.1. Sensor design

To verify the functioning of the separate sensor–actuator approach, a number of chips were designed. The general design with the corresponding chip is shown in Fig. 3. The design contains a large rectangular shaped actuator electrode around a double T shaped sensor electrode. This design was chosen to span a relatively large sensing area, preventing the measurement of local potentials as a result of Cl^- ion concentration differences over a large (non-interdigitated) sensor surface, while still keeping enough actuator electrode surface in between the fingers of the sensor. The sensor line width w and distance d between sensor and actuator were varied, resulting in chips with the values of Table 1. The minimum line width was the result of the constraints of the available fabrication technology. The sensor surface was chosen to be at least 200 times smaller than the actuator surface in order to deplete Cl^- near

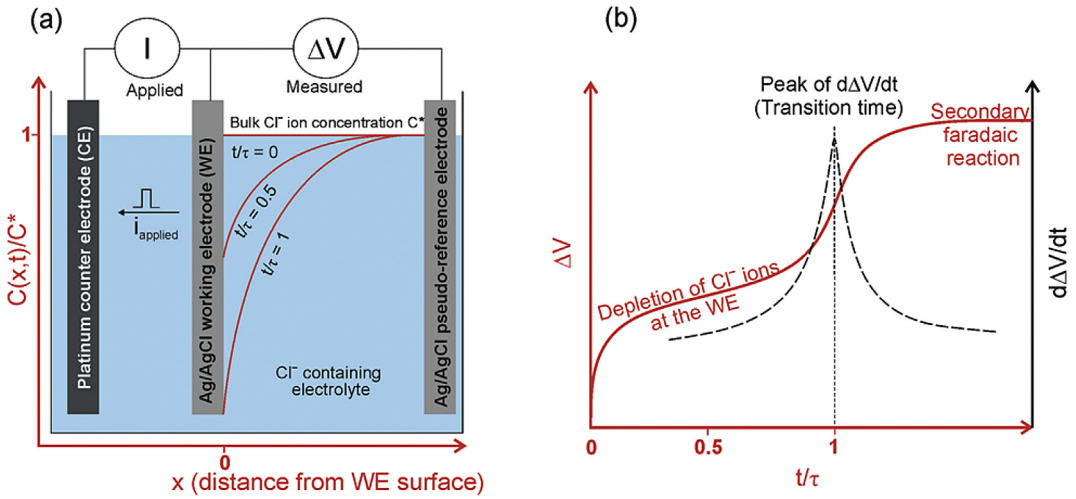

Fig. 1. (a) Normalized Cl^- concentration levels for different times t. A constant current is applied at $t > 0$. (b) Resulting potentiogram.

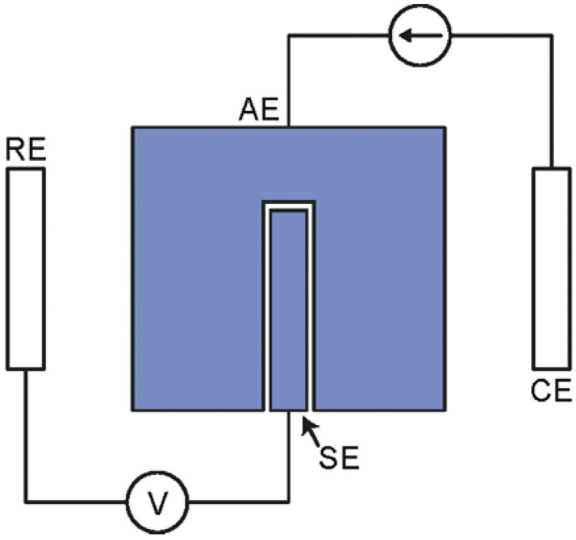

Fig. 2. Schematic representation of the electrode setup with separated sensor and actuator. RE = reference electrode, CE = counter electrode, SE = sensing electrode, AE = actuation electrode.

sensor surface.

3.1.1. Chip fabrication

The chips are fabricated using Borofloat glass wafers as substrate. The electrodes consist of a layered structure of 20 nm titanium, 40 nm platinum and 300 nm silver. Titanium is used as an adhesion promotor between the metal structures and the substrate. Platinum is used as a barrier to prevent diffusion between the titanium and the silver layer. The metals are sputtered into a recess etched into the substrate by a buffered hydrogen fluoride (BHF) solution, in such a way that the top of the metal structure will be level with the surface of the substrate.

Conventional lithography combined with a lift off process is used to pattern the metal layers. Parts of the chip are passivated by a polyimide (Durimide 7505), a polymer consisting of imide monomers, to cover the contact lines. Titanium is again used as an adhesion promotor, this time to improve the adhesion of the polyimide layer to the electrode, with again a platinum diffusion barrier in between. The full structure is shown in Fig. 4. The used polyimide is photosensitive and can therefore be patterned directly after spincoating the polymer on the surface. Metal areas not covered by the polyimide layer are then partly etched back to get to the silver surface. The detailed fabrication process along with the illustration is given in Supporting information S1.

After dicing the wafer, each chip is sonicated for five minutes in DI-water to remove glass particles from the dicing process. The chips were then stored in a clean environment. No chemical cleaning is performed as the cleaning process might affect the polyimide cover layer. Electroless deposition is then used to deposit AgCl on the silver electrodes as this gives the most uniform layer. Iron(III) chloride (ferric chloride, $FeCl_3$) is used in the following process:

$$Ag + FeCl_3 \rightarrow AgCl + FeCl_2 \quad (3)$$

A chip is secured in the experimental cell before 2 mL of 0.1 M ferric chloride solution is added. After 30 s, the solution is poured out and the chip is extensively rinsed with DI-water. The chip is dried using an air blow gun. Visual inspection verifies that the electrodes are covered by a gray layer. Color differences in this gray layer indicate a non-uniform layer and are a reason to reject some chips for experimental use.

3.2. Chemicals

Potassium chloride (KCl, BioXtra, ≥99.0%), potassium hydroxide (KOH, ≥90% pure reagent grade), potassium nitrate (KNO3, ReagentPlus®, ≥99.0%) and hexahydrated iron(III) chloride ($FeCl_36H_2O$, 98–102%) were obtained from Sigma–Aldrich, the Netherlands. Solutions were prepared using DI-water, deionized by a Millipore Milli-Q system.

3.3. Instrumentation and software

The experiments were conducted using a BioLogic SP-300 potentiostat controlled with BioLogic ECLab software (versions V10.31 and V10.32). For pH measurements, a Mettler Toledo SevenMulti was used in conjunction with a Mettler Toledo InLab 413 SG pH electrode. Sonication was performed by a VWR ultrasonic cleaner. MathWorks MATLAB R2012a (7.14.0.739) was used for data analysis and manipulation. Optical inspections were done using a Leica DM6000M optical microscope with Leica Application Suite 4.2.0 software.

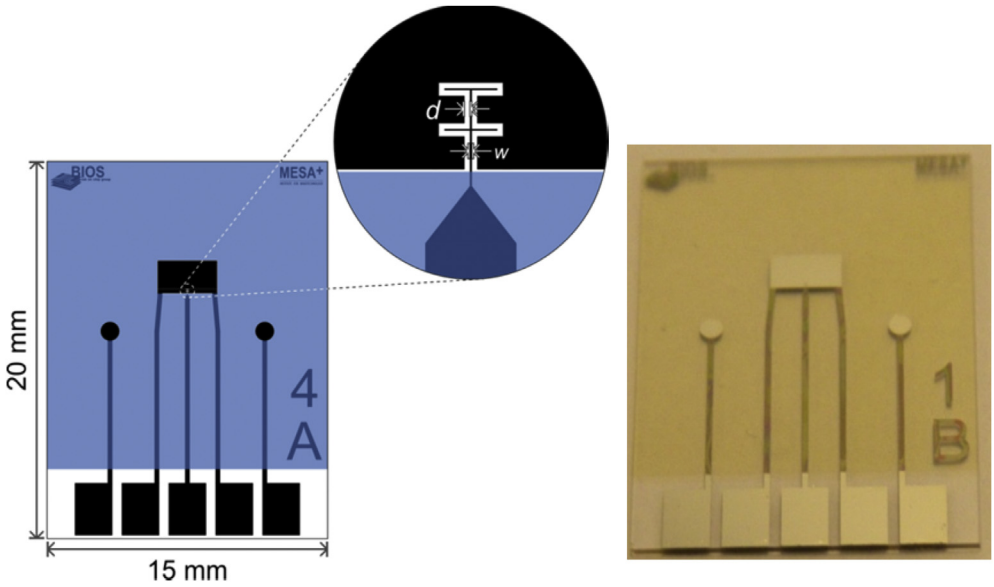

Fig. 3. Example of the chip design (image shows Design 4) with *d* the distance between sensor and actuator and *w* the line width of the sensor electrode. Two smaller electrodes are added for as pseudo-reference electrodes. The inset shows a close-up look of the design. Black structures are the silver electrodes, contact wires and contact pads, blue colored parts are insulated areas covered by a polyimide. On the right side, a photograph of a finished chip is shown. (For interpretation of the references to colour in this figure legend, the reader is referred to the web version of this article.)

Table 1
Specifications of the four different chip designs used in this work.

Chip design	Sensor line width (*w*) [μm]	Distance between sensor and actuator (*d*) [μm]	Sensor area [m^2]	Actuator area [m^2]
1	5	5	2.5×10^{-9}	5.4×10^{-6}
2	20	5	4.0×10^{-8}	8.5×10^{-6}
3	50	5	2.5×10^{-7}	1.6×10^{-5}
4	5	15	2.5×10^{-9}	5.6×10^{-6}

Fig. 4. Cross-section of the structure of the chip design. Shown thicknesses are not drawn to scale.

3.4. Experimental setup

The measurement setup consists of a custom-made Teflon experimental cell, in which one of the designed chips can be placed, as shown in Fig. 5a. The chip is electrically connected to the potentiostat through spring contacts. Besides the chip, two additional electrodes are placed inside the cell: a conventional Ag/AgCl reference electrode and a platinum counter electrode. Two measurement channels of the potentiostat are used in 'CE to ground'-mode and connected as visible in Fig. 5b. In this setup, the reference and counter electrodes are connected to both channels. The Pt CE electrode is placed in a lateral distance from the RE such that it does not come in between WE and RE. Apart from that, the information is in the transition time, rather than the absolute sensor potential.

The first channel is set up as a normal chronopotentiometric technique, in which a constant current is applied to the working electrode (WE). To prevent oxidation of the chips after local depletion of chloride, the potential is level limited. The second channel measures the potential of the sensor, 'SE'. All measurements are performed in a Faraday cage to prevent external influence on the measurement signal.

3.4.1. Chronopotentiometric response

A chip is secured into the chip holder and, unless otherwise noted, the electrochemical cell is filled with 5 mL of 1 mM KCl and 0.5 M KNO_3. Low chloride ion concentrations (in order of 1 mM) are chosen as higher current levels are required to deplete the higher concentration at the electrode surface (in the same time frame), which would degrade the actuator electrode (thin Ag film deposited over glass) faster. In this work, a current density of 10 A/m^2 is used, unless otherwise noted. For higher concentrations a thicker Ag/AgCl film should be used. This current density in combination

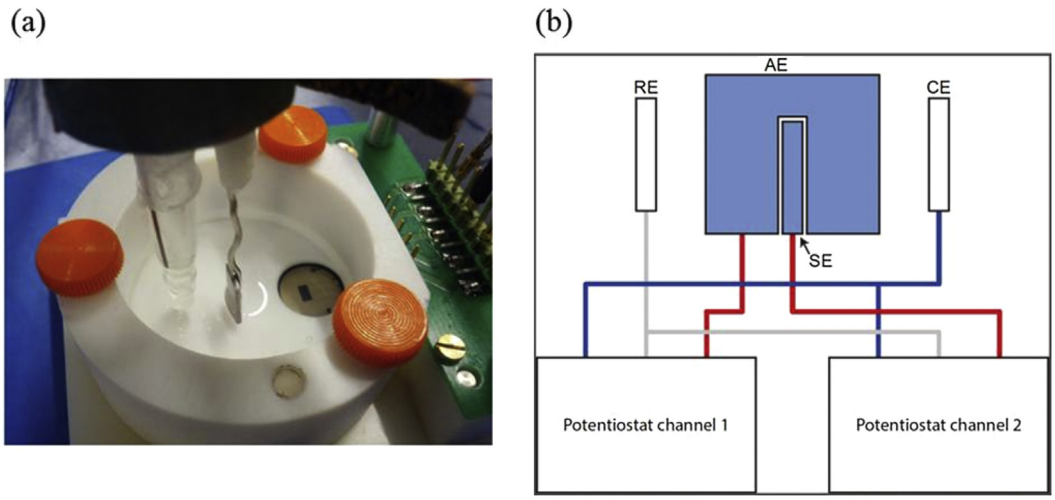

Fig. 5. (a) Schematic of the electrical connections to the electrochemical cell. RE = Ag/AgCl reference electrode, CE = Pt counter electrode, SE = on-chip sensing electrode, AE = on-chip actuator electrode. (b) Close-up picture of the chip holder. Inside the chip holder the electrodes are visible. From left to right: a Ag/AgCl reference electrode, a platinum counter electrode and the designed chip, inside the circular hole in the chip holder.

with the low concentration levels results in expected transition times within 10 s. Potassium nitrate acts as a background electrolyte to prevent migratory effects and to be able to regard this system as being diffusion controlled.

To increase the KCl concentration, a portion of the used solution is taken out and replaced by an equal volume of solution with higher KCl concentration. The KNO_3 concentration in both solutions is equal.

3.4.2. Measurement series

To characterize the designed sensor–actuator system, a number of experiments were performed. A calibration curve is obtained by measuring the sensor response for different Cl^- ion concentration levels. The series is measured from 1 mM to 6 mM Cl^- ion concentration in 1 mM steps in a solution containing 0.5 M KNO_3.

By comparing the calibration curves of chips with different line width w and distance d, the influence of these parameters can be investigated. The influence of current density applied to the actuator is investigated by a series of measurements in a solution with 3 mM KCl and 0.5 M KNO_3 by varying the current density from 3 A/m^2 to 10 A/m^2. According to the Sand equation, the transition time at the actuator should stay under 15 s in these cases, preventing convection having a significant influence on the system.

3.5. Data analysis

MATLAB is used to extract the transition time from the measurements. The data is filtered using a running average filter and the first derivative is taken. A maximum of this first derivative indicates the transition time, as illustrated in Fig. 6. The detailed algorithm and coding of the MATLAB program is given in Supporting information S2 and S3.

4. Result and discussion

4.1. Chronopotentiogram

Fig. 6 shows a typical chronopotentiogram for 3 mM KCl + 0.5 KNO_3 at 10 A/m^2 applied current pulse. Using the first derivative, the inflection point in other words the transition times can be determined. A running average filter is used to filter small signal variations due to white noise, which might result in a small time shift in the detected transition time.

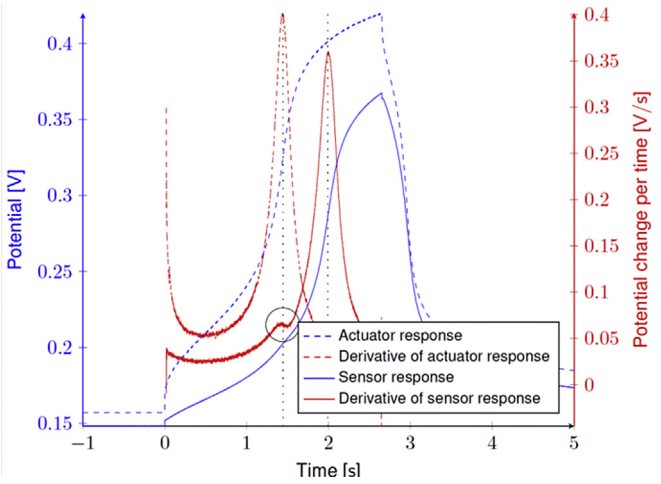

Fig. 6. Example of obtained chronopotentiogram from both sensor (solid blue line) and actuator (dashed blue line), with distance d of 5 μm and sensor line width w of 5 μm, after a current density of 10 A/m^2 is applied at $t > 0$. The solution contained 3 mM KCl and 0.5 M KNO_3. Derivatives of the (filtered) responses are shown for reference in red. The detected transition times are indicated by the black dotted lines. The circle indicates a small peak in the derivative, likely the result of crosstalk between the two electrodes. (For interpretation of the references to colour in this figure legend, the reader is referred to the web version of this article.)

Some measurement results show a small peak near the inclination point of the actuator response (indicated by a circle in Fig. 6). This is likely due to crosstalk through the solution between the two electrodes. The actuator signal shows an ohmic drop at the start of the current pulse (as is normal in chronoamperometric experiments). The sensor response also shows a small jump in the signal level, again likely caused by a resistive path between sensor and actuator.

4.2. Calibration curve

The sensor–actuator system is characterized by measuring the response for different Cl^- ion concentration levels. For reliable data, for each Cl^- ion concentration level, the measurements were

performed twice, while stirring the solution in between measurements to keep a constant Cl^- ion concentration throughout the solution. The measurement series run from 1 mM to 6 mM KCl in a solution also containing 0.5 M KNO_3. The resulting calibration curves are visible in Fig. 7. This concentration range (1–6 mM [Cl^-]) can be adapted by adjusting the applied current pulse [21]. Higher amplitude of the current is required for higher concentration range and vice versa.

The actuator response is very close to the theoretical curves. Based on a linear fit of the data, the actuator shows a diffusion coefficient of 2.38×10^{-9} m^2/s. This value is slightly above the reported value of 2.03×10^{-9} m^2/s found in literature [28]. However, the electrode area is not very well defined, as surface roughness might increase the effective area, which would lower the used current density and as a result from the Sand equation, change the slope of the calibration curve.

4.3. Effect of sensor size

The same measurement series, as was done for the calibration curves of Fig. 8, was repeated using a chip with $w = 20$ μm. For reliable measurement results, the chronopotentiometric measurement was performed twice for each Cl^- ion concentration level, after the solution was stirred in between measurements to assure a constant Cl^- ion concentration throughout the solution. The resulting measurement curve is visible in Fig. 8.

The transition times for the actuator with $w = 20$ μm are higher than expected. Since the current densities should be equal, the response should be closer to the Sand equation curve. Why this shift occurs is unclear; based on the figure one would expect that the concentration of KCl was off, but the same stock solution was used for both measurement series. Possibly, surface roughness increased the effective electrode area, resulting in a lower applied current density.

The difference between the transition time of the sensor and actuator is increased for the larger sensor (higher w). This behavior might be caused by the time it takes for the lowered Cl^- ion concentration (as a result of the current density applied at the actuator) to diffuse over the sensor. Since the sensor surface is larger, it takes more time before the concentration surface reaches a lower value, i.e. the concentration nearer to the actuator will be lower than the concentration at the center of the sensor. The observed sensor potential is therefore the result of a mixed potential across the sensor surface and it takes longer time to reach the inflection point typical for the transition time.

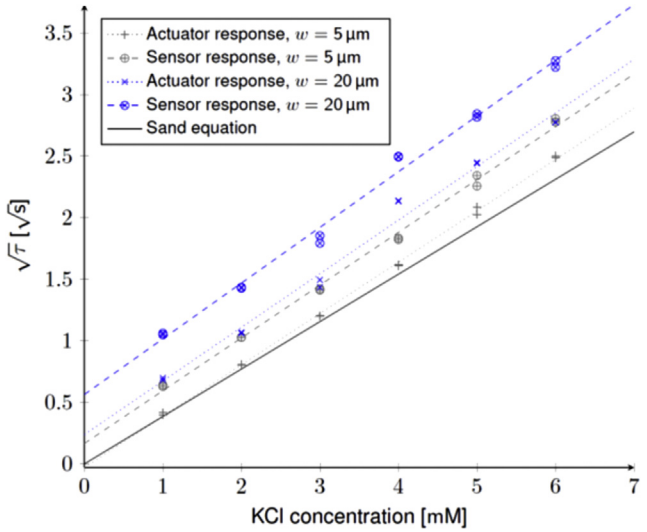

Fig. 8. Influence of sensor size on the transition time measurements of a sensor–actuator system. Two measurements were conducted for each KCl concentration in the range 1 mM–6 mM with a background electrolyte of 0.5 KNO_3. The sensor–actuator system had $d = 5$ μm and $w = 20$ μm and a current density of 10 A/m^2 was used. For comparison, the results of a sensor actuator system with $d = 5$ μm and $w = 5$ μm are included in the graph.

4.4. Effect of distance between sensor and actuator

Besides line with w, also the distance d between sensor and actuator was varied. The same measurement series, as was done for the calibration curves of Fig. 8, was repeated using a chip with $d = 15$ μm. For reliable measurement results, the chronopotentiometric

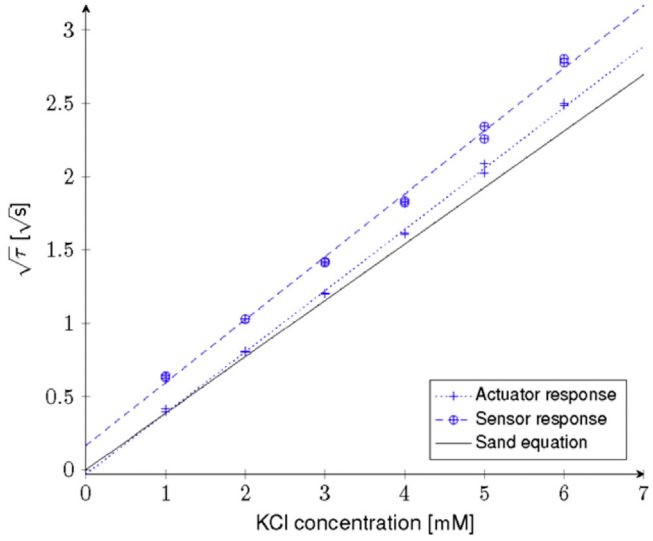

Fig. 7. Calibration curves of a sensor–actuator system. Two measurements were conducted for each KCl concentration in the range of 1 mM–6 mM with a background electrolyte of 0.5 M KNO_3. The used sensor–actuator system has $d = 5$ μm and $w = 5$ μm and a current density of 10 A/m^2 was used.

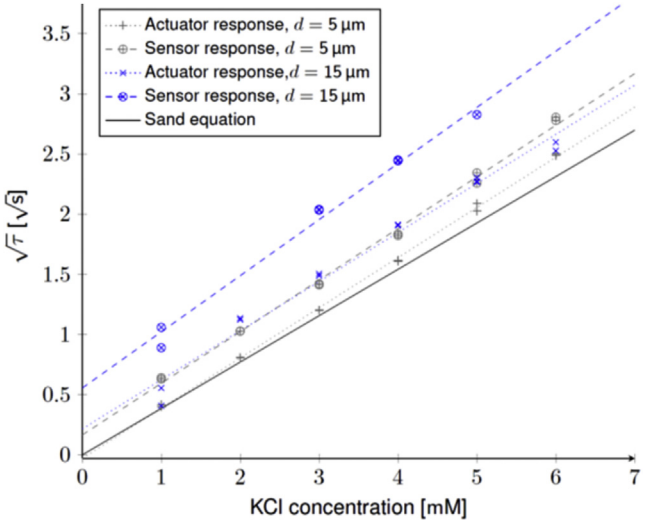

Fig. 9. Influence of distance d between sensor and actuator. Two measurements were conducted for each KCl concentration in the range 1 mM to 6 mM with a background electrolyte of 0:5M KNO_3. The sensor–actuator system had $d = 15$ μm and $w = 20$ μm and a current density of 10 A/m^2 was used. For comparison, the results of a sensor–actuator system with $d = 5$ μm and $w = 5$ μm are included in the graph.

measurement was performed twice for each Cl^- ion concentration level, after the solution was stirred in between measurements to assure a constant Cl^- ion concentration throughout the solution. The resulting measurement curve is visible in Fig. 9.

Just as in the previous measurement results, the transition times observed at the actuator are higher than expected. The observed sensor signals did not result in transition time detections for every measurement. In these cases, no inflection point was reached before the current pulse was ended to prevent further oxidation of the actuator. The larger distance between sensor and actuator gives more chance for unwanted effects, such as convection, to occur.

In cases where successful detection was possible, an increase in time between the transition at the sensor and actuator was observed. This behavior could be caused by the diffusion profile expanding in such a way that it takes a significant amount of time before a concentration change reaches the sensor as the distance d between the two electrodes has to be covered first.

4.5. Effect of current density

According to the Sand equation (eq. (2)), the transition time is dependent on the current density. To verify this behavior, a measurement series was performed with a chip with $w = 5$ μm and $d = 5$ μm in a solution containing 3 mM KCl and 0.5 M KNO_3, while varying the current density from 3 A/m^2 to 10 A/m^2 in 1 A/m^2 steps. For each current density, the measurement was repeated after stirring the solution.

Fig. 10 shows the square root of the obtained transition time versus the reciprocal of the current density, which should result in a straight line according to the Sand equation. By changing the current density, the sensitivity of the system can be changed since the transition time can be shifted by applying a different current density, i.e. making sure that the transition time occurs within a certain time frame.

4.6. Comparison of separated and combined sensor–actuator

The purpose of the separated sensor–actuator electrode is to enhance the lifetime of the sensor electrode by using a separated actuator as a sacrificial electrode. The transition time measurement of the combined and separated sensor–actuator electrode is shown in Fig. 11. In case of the combined sensor–actuator a current pulse is applied to the sensor electrode and its potential is measured simultaneously. Relatively long current pulses were applied and 20 measurements were performed to simulate the long-term character. A current pulse of 10 μA/cm^2 is applied for 5 s in an electrolyte containing 1 mM Cl^- concentration. After 14 measurements the transition time of the combined sensor–actuator increases drastically from 0.1 to ca. 10 s. The transition time does not correspond to the Cl^- ion concentration anymore. Whereas for the separated sensor–actuator, the responses are repeatable for the same number of measurements and more. This indicates the improved long-term behavior of the separated over the combined sensor–actuator.

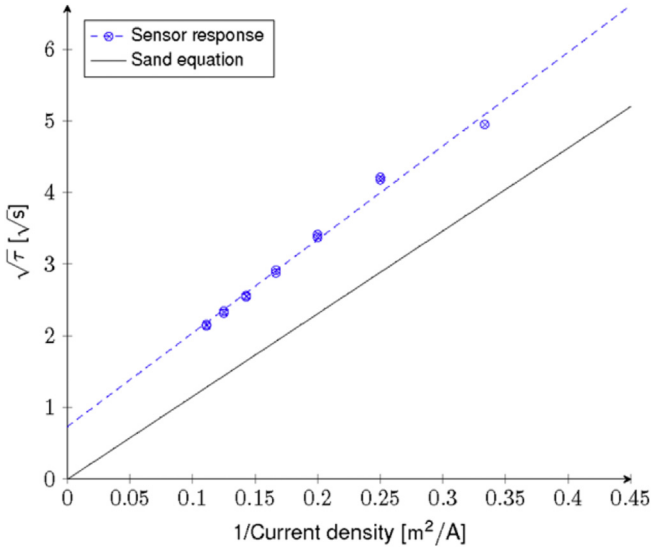

Fig. 10. Influence of current density on measured transition times, plotted as the square root of transition time versus the reciprocal of the current density to obtain a linear relationship. Two measurements were conducted for each current density in the range of 3 A/m^2 to 10 A/m^2 in a solution containing 3 mM KCl and 0.5 M KNO_3. The used sensor–actuator chip had $d = 5$ μm and $w = 5$ μm.

5. Conclusion

The aim of this work is to give a proof of concept of a separated sensor–actuator system for dynamic measurement of Cl^- ions. The performed experiments showed that the sensor indeed senses the local concentration changes resulting from the current applied to the actuator. A linear relation between concentration and the square root of the transition time was observed at the actuator, as predicted by the Sand equation (Equation (2)). The sensor showed the same linear relation, but an additional delay was observed between the sensor and actuator signal.

The variation of design parameters resulted in a few observations. First of all, the distance (d) between the two electrodes should be small. A larger distance resulted in less reliable detections of the transition time and an increase in the delay between the transition time at the sensor and actuator. Secondly, a larger sensor area (by increasing line width w) resulted in an increase of the transition time as observed at the sensor.

Variation of the applied current density resulted in a change of the transition time according to and as expected from the Sand equation. Increasing the current density results in a decrease of the transition time and vice versa. This could be used to tune the sensitivity of the sensor–actuator system.

The introduced separated sensor–actuator approach opens the door for chronopotentiometric measurements in cases where current passing the sensor electrode is undesirable. The proposed method of dynamic measurement removes the need for a conventional reference electrode and can thus be applied in long-term

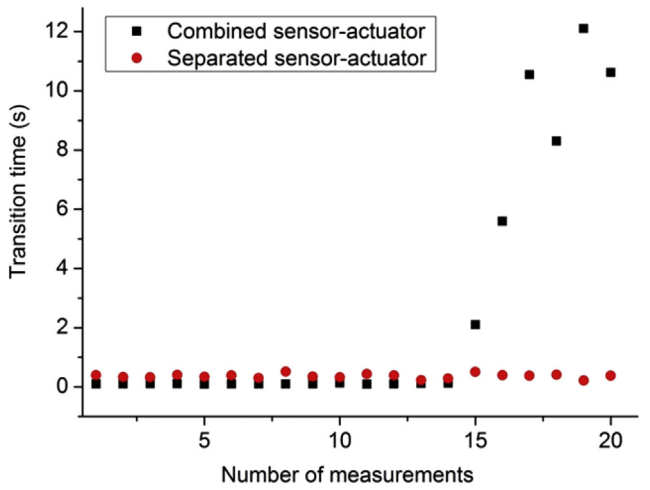

Fig. 11. Comparison of the combined and separated sensor actuator. For both cases transition times are measured for 20 cycles in 1 mM Cl^- ion concentration at an applied current of 10 A/m^2 for 5 s.

applications such as [Cl^-] monitoring in concrete. The sensor should be calibrated first in a concrete sample as the diffusion coefficient of Cl^- in concrete is different from that in aqueous electrolyte tested in this work. Other application includes monitoring of Cl^- and other halide ions (pollutant) in physiological solution and in drinking water. The introduced separation of the sensing and actuating electrode decreases the possibility of failure of the proposed system: the two distinct sensor and actuator sub systems can now be individually optimized, making long-term applications even more feasible.

Acknowledgment

This work is a part of STW project “Integral solution for sustainable construction (IS2C, http://is2c.nl/project-10968/)”. We are grateful to the STW Netherlands for their financial support.

Appendix A. Supplementary data

Supplementary data related to this article can be found at http://dx.doi.org/10.1016/j.aca.2015.06.047.

References

[1] A. Martin, R. Narayanaswamy, Studies on quenching of fluorescence of reagents in aqueous solution leading to an optical chloride-ion sensor, Sensors Actuat. B Chem. 39 (1997) 330–333.
[2] J.N. Babu, V. Bhalla, M. Kumar, R. Mahajan, R.K. Puri, A chloride selective sensor based on a calix [4] arene possessing a urea moiety, Tetrahedron Lett. 49 (2008) 2772–2775.
[3] C. Huber, I. Klimant, C. Krause, T. Werner, T. Mayr, O.S. Wolfbeis, Optical sensor for seawater salinity, Fresenius' J. Anal. Chem. 368 (2000) 196–202.
[4] J.P. Broomfield, Corrosion of Steel in Concrete: Understanding, Investigation and Repair, CRC Press, 2002.
[5] B. Elsener, H. Bohni, Potential Mapping and Corrosion of Steel in Concrete, in: Corrosion Rates of Steel in Concrete, vol. 1065, ASTM STP, 1990, pp. 143–156.
[6] U. Angst, B. Elsener, C.K. Larsen, Ø. Vennesland, Potentiometric determination of the chloride ion activity in cement based materials, J. Appl. Electrochem. 40 (2010) 561–573.
[7] G. Loreto, M. Di Benedetti, R. Iovino, A. Nanni, M. Gonzalez, Evaluation of corrosion effect in reinforced concrete by chloride exposure, in: SPIE Smart Structures and Materials+ Nondestructive Evaluation and Health Monitoring, 2011, pp. 79830A-A-79830A-10.
[8] A. Moncmanová, Environmental Deterioration of Materials, vol. 21, WIT Press, 2007.
[9] F. He, C. Shi, Q. Yuan, C. Chen, K. Zheng, $AgNO_3$-based colorimetric methods for measurement of chloride penetration in concrete, Constr. Build. Mater. 26 (2012) 1–8.
[10] D.D. Van Slyke, The determination of chlorides in blood and tissues, J. Biol. Chem. 58 (1923) 523–529.
[11] Y. Abbas, W. Olthuis, A. van den Berg, A chronopotentiometric approach for measuring chloride ion concentration, Sensors Actuat. B Chem. 188 (2013) 433–439.
[12] M.A. Climent-Llorca, E. Viqueira-Pérez, M.M. López-Atalaya, Embeddable Ag/AgCl sensors for in-situ monitoring chloride contents in concrete, Cem. Concr. Res. 26 (1996) 1157–1161.
[13] R. Myrdal, The Electrochemistry and Characteristics of Embeddable Reference Electrodes for Concrete, Woodhead Publishing, 2014.
[14] E. Bakker, V. Bhakthavatsalam, K.L. Gemene, Beyond potentiometry: robust electrochemical ion sensor concepts in view of remote chemical sensing, Talanta 75 (2008) 629–635.
[15] W. Olthuis, G. Langereis, P. Bergveld, The metrits of differential measuring in time and space, Biocybern. Biomed. Eng. 21 (2001) 5–26.
[16] K.L. Gemene, A. Shvarev, E. Bakker, Selectivity enhancement of anion-responsive electrodes by pulsed chronopotentiometry, Anal. Chim. Acta 583 (2007) 190–196.
[17] M. Cuartero, G.A. Crespo, M. Ghahraman Afshar, E. Bakker, Exhaustive thin-layer cyclic voltammetry for absolute multianalyte halide detection, Anal. Chem. 86 (2014) 11387–11395.
[18] W. Olthuis, J. Bomer, P. Bergveld, M. Bos, W. Van der Linden, Iridium oxide as actuator material for the ISFET-based sensor-actuator system, Sensors Actuat. B Chem. 5 (1991) 47–52.
[19] K.L. Gemene, E. Bakker, Direct sensing of total acidity by chronopotentiometric flash titrations at polymer membrane ion-selective electrodes, Anal. Chem. 80 (2008) 3743–3750.
[20] P. Bergveld, J. Eijkel, W. Olthuis, Detection of protein concentrations with chronopotentiometry, Biosens. Bioelectron. 12 (1997) 905–916.
[21] Y. Abbas, D.B. de Graaf, W. Olthuis, A. van den Berg, No more conventional reference electrode: transition time for determining chloride ion concentration, Anal. Chim. Acta 821 (2014) 81–88.
[22] R. Iwamoto, Derivative chronopotentiometry, Anal. Chem. 31 (1959) 1062–1065.
[23] A.J. Bard, L.R. Faulkner, Electrochemical Methods: Fundamentals and Applications, second ed., Wiley and Sons, Hoboken, 2001.
[24] R.E. Meyer, F.A. Posey, P.M. Lantz, Chronopotentiometry of the Ag–AgCl system and analysis for the chloride ion, J. Electroanal. Chem. Interfacial Electrochem. 19 (1968) 99–109.
[25] W. Olthuis, P. Bergveld, Simplified design of the coulometric sensor–actuator system by the application of a time-dependent actuator current, Sensors Actuat. B Chem. 7 (1992) 479–483.
[26] W. Olthuis, P. Bergveld, Integrated coulometric sensor-actuator devices, Microchim. Acta 121 (1995) 191–223.
[27] G.J. Janz, D.J. Ives, Silver, silver chloride electrodes, Ann. N. Y. Acad. Sci. 148 (1968) 210–221.
[28] E.L. Cussler, Diffusion: Mass Transfer in Fluid Systems, Cambridge University Press, 2009.